BISTATIC RADAR OBSERVATIONS OF A SAMPLE OF LUNAR PYROCLASTIC DEPOSITS. S. S. Bhiravarasu[1], P. A. Taylor[1], E. G. Rivera-Valentín[1, 2], A. K. Virkki[1], G. W. Patterson[3], J. T. S. Cahill[3] and M. C. Nolan[4]; [1]USRA/Arecibo Observatory, Arecibo, PR (sbhiravarasu@usra.edu), [2]USRA/Lunar and Planetary Institute, Houston, TX, [3]Johns Hopkins Applied Physics Laboratory, Laurel, MD, [4]University of Arizona, LPL, Tucson, AZ.

Introduction: Lunar pyroclastic volcanism represents an important aspect of volcanic activity on the Moon. Pyroclastic deposits are globally distributed, but are most frequently observed in the highlands adjacent to major Maria or along fissures within floor-fractured craters [1, 2]. Large (over 2500 km^2) pyroclastic deposits are thought to have formed from long-duration fire fountaining accompanying basaltic volcanism, while smaller pyroclastic deposits were more likely emplaced through episodic volcanic events [2, 3]. Lunar localized pyroclastic deposits (with areas < 2500 km^2) have been difficult to study because of a lack of available data with sufficiently high spatial-resolution.

The low radar backscatter coupled with low circular polarization ratio (CPR) values associated with fine-grained pyroclastic material provide a useful method of distinguishing fine-grained volcanic material from optically dark Maria including the radar dark high-titanium basalts [3, 4]. Here, we utilize bistatic radar data acquired at S- and X-bands, along with ground-based radar and other spacecraft data sets, to characterize the physical properties of several localized pyroclastic deposits.

Summary of Datasets used: In this study, we used and integrated several data sets from various instruments on LRO and ground-based radar systems. The Mini-RF instrument aboard NASA's LRO is a hybrid dual-polarized synthetic aperture radar (SAR) that operates at both S-band (12.6 cm) and X-band (4.2 cm). During the exploration phase of the mission, Mini-RF mapped 2/3 of the lunar surface at S-band using a monostatic architecture with a nominal incidence angle of 49° and a resolution of 15×30 m/pixel [5]. Toward the end of the initial science phase of the mission, the Mini-RF transmitter experienced a malfunction and ceased to operate, precluding further monostatic data collection. However, Mini-RF resumed operations starting in the 1st LRO extended mission and has worked in concert with the Arecibo Observatory (AO) and the Goldstone deep space communications complex 34 meter antenna DSS-13 to collect S- and X-band bistatic radar data of the Moon [6, 7]. The primary goal of the Mini-RF bistatic campaign is to observe the scattering characteristics of the upper meter(s) of the lunar surface, as a function of bistatic angle, for a variety of terrain types to search for and characterize the presence of an opposition response [6-9]. The resolution of the bistatic Mini-RF data is ~100 m in range and ~2.5 m in azimuth, but can vary from observation to observation, as a function of the viewing geometry. For this analysis, the data are averaged in azimuth (~40 looks) to provide a spatial resolution of 100 m.

Along with the monostatic (S-band) and bistatic (S- and X-bands) Mini-RF data, we have utilized both S-band (80 m/pixel) and P-band (400 m/pixel) ground-based AO-GBT (Green Bank Telescope) radar data to study the extent and distribution of the pyroclastic deposits. To understand the variation of radar CPR with the surface rock abundance (RA) and TiO_2 content, we used global 128 ppd maps of Diviner rock abundance [10] and TiO_2 maps derived from the global LROC WAC UV-Vis data (at 64 ppd ~ 473 m/pix) using the methods of [11].

Montes Carpatus region: Pyroclastic deposits in the vicinity of Montes Carpatus occur as irregular patches, either within the highlands or on the maria adjacent to the highlands [12]. Monostatic S-band radar data of one such patch (19.2°N, 31.1°W) clearly indicate a very dark deposit that mantles the highland blocks (Fig. 1b) with average CPR value of 0.53±0.21. Mini-RF bistatic X-band data covering the eastern part of the deposit

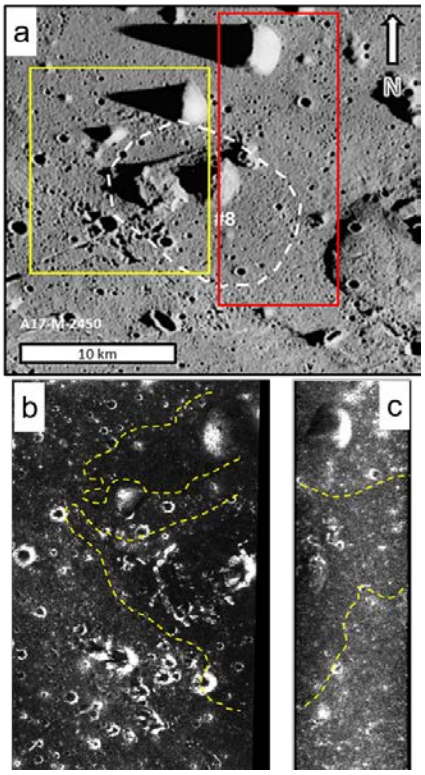

Figure 1 *a) Portion of Apollo orbital photo A17-M-2450 for Montes Carpatus showing a pyroclastic deposit with approximate boundary outlined in a white polygon (Fig. 18 (b) of [12]). Yellow and Red boxes show the extent of Mini-RF (b) S-band monostatic and (c) bistatic X-band S_1 images respectively. The extent of dark mantled pyroclastic deposits are outlined in yellow in (b) and (c).*

(Fig. 1c) also show a dark region separated from the background regolith with average CPR value of 0.35±0.10 (mean bistatic angle of 6.5° and incidence angle of 39.3°). The average CPR values for the total extent of this deposit (as in Fig. 1a) in AO S- and P-band radar data are 0.47±0.12 and 0.27±0.09 respectively, observed at incidence angles of 36.8° and 45°. Differences between CPR values at different wavelengths can be caused by variations in material size or burial depth [3]. The enhanced CPR values observed in S- band radar data indicates contamination from adjacent blocky crater ejecta towards the western part of the deposit or partly due to the presence of bright rays (apparently superimposed) of highland debris from Copernicus crater. No enhancement in the P-band radar CPR, combined with the low RA values (in the range of 0.003) indicates that the blocks are too small to be resolved by the longer-wavelength P-band signals. However, this doesn't explain the low CPR values observed from the eastern part of this deposit from bistatic X-band radar data.

Sinus Iridum region: The Sinus Iridum region is host to many geological events (from pre-Imbrium to Copernican era), shaped by long-lived lunar volcanism [13]. Mini-RF has made bistatic observations that include part of Iridum crater at both S- and X-band wavelengths. The bistatic S-band radar data show a very dark region surrounding the crater Heraclides E, discernable in both S1 and CPR images (outlined in Fig. 2 a and b). This observation of Iridum dark mantled deposit cover bistatic angles of 4.1° to 6.4° for incidence angles ranging from 55.2° to 58.5°. This region has an average CPR value of 0.37±0.12 (measured away from craters), and is clearly distinguishable from the adjacent optically dark mare having average CPR values in the range of 0.48±0.13. X-band bistatic data of the region (at bistatic angles of 3.2° to 5.1° for incidence angles ranging from 54.6° to 57°), do not show a clear, uniform boundary with the surrounding mare. The monostatic S-band Mini-RF and AO S-band radar data doesn't cover this region. The average CPR value obtained from AO P-band radar data (at inc. angle of 59°) of this deposit is 0.31±0.09. The corresponding average values of RA and TiO_2 observed within this deposit are 0.003±0.001 and 5.1±0.69 wt. % respectively. The sharp boundary observed in S-band radar data is not clearly visible in the P-band radar, TiO_2 and RA datasets, most possibly due to their low spatial resolution. If this dark region has been partially mantled by fine-grained, rock poor pyroclastics, it would be another example of a localized pyroclastic deposit surrounding a source vent/dome on a relatively flat mare surface similar to those observed in [12]. Also, the slightly enhanced TiO_2 values indicate that this source vent might have produced pyroclastic mantling deposits of basaltic composition.

Summary: We present preliminary results obtained from the analysis of recent Mini-RF radar bistatic observations. When combined with monostatic radar observations, bistatic radar data at different incidence and phase angles offer a different viewing geometry of the surface, which allows comparisons of the radar backscatter between localized pyroclastic deposits. Multiwavelength radar data can also be useful for determining which areas of pyroclastic deposits are contaminated by crater ejecta, and which areas are thinner. We will continue analyzing bistatic radar data of the Moon in an effort to understand the physical properties of various lunar terrains as a function of phase angle at multiple wavelengths.

References: [1] Gaddis et al. (1985), *Icarus*, 61, 461-489; [2] Wilson and Head (1981), *JGR*, 86, 2971-3001; [3] Carter et al. (2009), *JGR*, 114, E11004; [4] Trang et al. (2017), *Icarus* 283, 232-253; [5] Cahill et al. (2014), *Icarus* 243, 173-190; [6] Patterson et al. (2017), *Icarus* 283, 2-19; [7] Patterson et al. (2017), *LEAG 2017*, Abs #5046; [8] Hapke et al. (2012), *JGR*, 117, E00H15; [9] Hapke and Blewett (1991), *Nature*, 352, 46-47; [10] Bandfield et al. (2011), *JGR*, 116, E00H02; [11] Sato et al. (2015), *46th LPSC*, Abs #1111; [12] Gustafson et al. (2012), *JGR*, 117, E00H25; [13] Chen et al. (2010), *Science China*, 53, 2179-2187.

Acknowledgements: This material is based upon work supported by NASA through the LRO Mini-RF under Grant No. NNN06AA01C. The Arecibo Observatory Planetary Radar program is fully funded by NASA through the Near-Earth Object Observations program under Grant Nos. NNX12AF24G and NNX13AQ46G awarded to USRA.

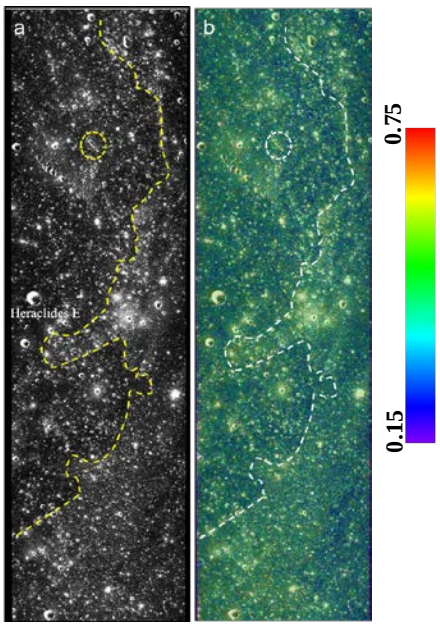

Figure 2 *S-band bistatic radar data for a portion of Sinus Iridum. Possible boundary between pyroclastic deposit and mare is indicated with a dashed line in both [a] total backscattered power (S_1) and [b] CPR images. The CPR image is overlaid on S_1 and stretched from 0.15 to 0.75 (color bar). North is to the top and the crater Heraclides E 43°N, 32.76°W) is labled in (a). A source vent / dome is indicated in a dashed circle in both (a) and (b).*